

Article

Dynamic Properties of Calcareous Sands from Urban Areas of Abu Dhabi

Ahmed Khalil, Zahid Hamid Khan , Mousa Attom, Magdi El Emam  and Kazi Fattah 

Department of Civil Engineering, American University of Sharjah, Sharjah P.O. Box 26666, United Arab Emirates; b00079152@aus.edu (A.K.); mattom@aus.edu (M.A.); melemam@aus.edu (M.E.E.); kfattah@aus.edu (K.F.)

* Correspondence: zhkhan@aus.edu; Tel.: +971-(0)-6515-2926

Abstract: Abu Dhabi (ABD) has recently developed its national building code that mandates dynamic analysis of large structures to seismic loadings. Large strain dynamic properties such as shear modulus (G) and damping ratio (D) of local undisturbed calcareous sands are not available. Designers are compelled to choose degradation models from studies on calcareous sands of other regions that are usually reconstituted. This research presents for the first time large strain dynamic properties of calcareous sands of urban ABD. Undisturbed samples are collected from different areas of urban ABD and are tested in cyclic triaxial (CT) devices fitted with bender elements (BE). The dynamic properties as functions of confinement are curve fitted with power models, whereas their variation with shear strain level is curve fitted with hyperbolic models. The results are compared with findings of previous studies on calcareous and silica sands. The results indicate that dynamic properties of all samples degrade with shear strain at almost the same rate irrespective of their spatial distribution. The proposed degradation models can therefore be used in dynamic analyses. The results from this study show smaller rates of degradation in dynamic properties compared to other studies on similar sands. The change in low-strain shear wave velocity (V_s) with confinement is significant among the tested samples; therefore, a site-specific evaluation of V_s is recommended. The dynamic properties of calcareous sands of ABD and previous studies however exhibit larger degradation with shear strain and a smaller increase in confinement compared to silica sands.

Keywords: calcareous sands; cyclic triaxial; bender elements; shear modulus; damping ratio; United Arab Emirates



Citation: Khalil, A.; Khan, Z.H.; Attom, M.; El Emam, M.; Fattah, K. Dynamic Properties of Calcareous Sands from Urban Areas of Abu Dhabi. *Appl. Sci.* **2022**, *12*, 3325. <https://doi.org/10.3390/app12073325>

Academic Editor: Tiago Miranda

Received: 23 February 2022

Accepted: 22 March 2022

Published: 24 March 2022

Publisher's Note: MDPI stays neutral with regard to jurisdictional claims in published maps and institutional affiliations.



Copyright: © 2022 by the authors. Licensee MDPI, Basel, Switzerland. This article is an open access article distributed under the terms and conditions of the Creative Commons Attribution (CC BY) license (<https://creativecommons.org/licenses/by/4.0/>).

1. Introduction

Abu Dhabi (ABD) in the United Arab Emirates (UAE) has recently developed a national building code [1] to support the significant growth in the construction sector. The code mandates dynamic analysis of structures under seismic loading, which requires the dynamic properties of subsurface material as a function of shear strain level among other geotechnical properties. The behavior of dynamic properties of soils such as the shear modulus (G) and the damping ratio (D) at different shear strain levels are typically obtained from laboratory tests. Since the Cambrian age, the region of ABD has primarily consisted of sediments deposited mostly from Tertiary rocks of a shallow shelf environment (carbonate platform). Recent sediment deposits in and around ABD are rich in carbonate minerals with varying amounts of gypsum and seashells. The reclaimed areas along the shores of ABD are also constructed with dredging and hydraulic fills of calcareous sands from the Arabian Gulf (Kirkham [2]). The dynamic characterization of these soils is expected to be significantly different not only from siliceous sands but also from calcareous sands of other regions.

Several studies have evaluated the dynamic properties for silica sands with bender element (BE), cyclic triaxial (CT) and resonant column (RC) tests (e.g., Cascante et al. [3]; Khan et al. [4]; Khan et al. [5]; Irfan et al. [6]). Similarly, several studies are available

for reconstituted samples of calcareous sands found in geographical regions other than ABD (Carraro and Bortolotto [7]; Fioravante et al. [8]; Jafarian et al. [9]; Liu et al. [10]; Van Impe et al. [11]). One study evaluated the dynamic properties of reconstituted samples of naturally occurring calcareous sands of ABD (Giang et al. [12]); however, it did not evaluate the dynamic properties as a function of shear strain. Similarly, Giretti et al. [13] also tested reconstituted samples obtained from a hydraulic fill of an island close to ABD. The designers in ABD typically rely on degradation models of dynamic properties that are not representative of regional soils for the purpose of site response analysis. The focus of this study is to evaluate the dynamic properties of in situ undisturbed calcareous sands of ABD as a function of shear strain level and to present the results in the form of standard hyperbolic models for dynamic analyses. Undisturbed specimens of calcareous sands are collected from different zones of urban ABD. The dynamic properties are evaluated at different confinements and shear strain levels in cyclic triaxial (CT) devices fitted with bender elements (BE). The low strain V_s is obtained from bender element (BE) tests. The results are fitted with hyperbolic models (Hardin and Drenevič [14]) and then compared with selected studies on calcareous and siliceous sands from the literature.

The results indicate that sands from urban areas of ABD degrade less than calcareous sands of other regions mainly because of reconstitution of the sands in those studies that can damage the effective inter-particle cementation. The variation of V_s with confinement shows large variability among the tested sands in the present study, and it is therefore recommended to evaluate low-strain properties on a case-by-case basis. The degradation behavior of the tested sands appears to be unaffected by the source or location of the material within ABD. The presented hyperbolic models can therefore be used for site response analysis or soil structure analysis as mandated by the national building code of ABD.

2. Background and Literature

Carraro and Bortolotto [7] presented results from resonant column testing on the evaluation of stiffness and damping of calcareous and siliceous sands. They tested two reconstituted sand samples that were retrieved from Northwest Australia. Both samples had the same state density and particle size distribution. Six confinements (50, 100, 200, 400, 800 and 1600 kPa) were used. The results indicated higher dynamic properties as well as faster stiffness degradation for calcareous sand compared to silica sand.

Jafarian et al. [9] presented results from CT and RC tests on calcareous and siliceous sand samples from the Bushehr region of the Arabian Gulf. A total of 36 tests were conducted. Bushehr sand is classified as calcium carbonate (CaCO_3) comprising 53.1% of sample volume. Scanning electron microscopic (SEM) images showed angular and sub-angular soil particles with a rough surface. Bushehr sand is blended with transported soil and biological carbonate materials. It is classified as a poor graded sand (SP). The main objective was to assess the effect of the mean confinement, sample density, and stress anisotropy on the dynamic properties (i.e., shear modulus and damping ratio). The effect of the initial stress anisotropy was insignificant to the dynamic properties; however, the variation of initial mean confinement and relative density showed significant effects.

Liu et al. [10] conducted a series of resonant column tests on reconstituted carbonate and siliceous sands samples. All cylindrical samples had dimensions of 50 by 100 mm. The samples were taken from the South China Sea (Jinzhong region). They presented the dynamic properties (shear modulus and damping ratio) for nine samples from each sand type. The main focus of the study was to evaluate the effects of different initial relative densities and different confinements on dynamic properties. The relative density for the 18 samples ranged from 38.6% to 72.7%, while three isotropic effective confinements of 29, 57 and 97 kPa were used. They noticed higher dynamic properties at low strains but faster stiffness degradation for calcareous sand compared to siliceous sand.

Giang et al. [12] evaluated the shear modulus of two types of sands with BE, which were collected from different locations of ABD and the Belgian province of Antwerp. In

their study, they tested several reconstituted cylindrical samples (50 by 90 mm) of calcareous and silica sands. The main focus of the study was to investigate and compare the effects of particle shape on dynamic properties. The results indicated a higher shear modulus in calcareous sands compared to silica sands at low strains. The results only presented variations of Vs with confinements and did not show degradation characteristics.

Giretti et al. [13] presented the results of a comprehensive laboratory testing program, which included BE, CT, and RC tests. Samples were collected from the hydraulic fill of an artificial island located in the UAE. The fill mainly comprised calcareous sand, which was predominantly aragonite. A total of 37 reconstituted drained and undrained samples were tested. The small-strain Vs and the compression wave velocity (Vp) were measured with BE (30 to 1200 kPa). The results of the RC testing were in good agreement with the results from Fioravante et al. [8] and Van Impe et al. [11].

Morsy et al. [15] showed the evaluation of dynamic properties for representative calcareous sand from a newly developed coastal area near the Mediterranean Sea. Tests were performed with a resonant column (RC) to study the effect of the void ratio, saturation, particle shape and confinement on the measured dynamic properties. The study showed that the shear modulus was higher for calcareous sand at higher confinements compared to the shear modulus for siliceous sands.

Various models have been proposed in the literature to curve-fit the measured dynamic properties as a function of shear strain level. Hardin [16] proposed a hyperbolic model to describe the nonlinear soil behavior under cyclic loading. The hyperbolic model presented by Hardin [16] generally results in a poor fit to the test data because it involves one curve-fitting parameter. A modified hyperbolic model suggested by Hardin and Drnevich [14] provides superior fit to the data, as shown in Equation (1).

$$\frac{G}{G_{max}} = \frac{1}{1 + \gamma_h} \quad (1)$$

where G_{max} is the shear modulus measured at lowest possible strain levels, G is the shear modulus measured at higher strain levels, and γ_h is the hyperbolic strain defined by Equation (2).

$$\gamma_h = \frac{\gamma}{\gamma_r} \left(1 + a \exp \left(-b \frac{\gamma}{\gamma_r} \right) \right) \quad (2)$$

where γ_r is the reference shear strain indicating the beginning of non-linear behavior, and a and b are the curvature coefficients of the model. A similar equation is also proposed for modeling the variation of the damping ratio (D) with shear strain level, as shown in Equation (3)

$$\frac{D}{D_{max}} = \frac{\gamma_h}{1 + \gamma_h} \quad (3)$$

where D_{max} is the maximum damping ratio that corresponds to minimum G . The time domain method, despite its limitations, is easier to use than the frequency domain method for the evaluation of low strain Vs in BE testing. The accuracy of the frequency domain method relies on π -point identification. Although the frequency domain is superior to the time domain, it consumes more time, and only a limited number of π -points can be recorded, as it requires manual sweeping (Brocanelli [17]; Camacho-Tauta [18]). Moreover, Irfan et al. [6] and Cristiana et al. [19] showed that the actual response of the embedded bender element is different from the electronic record of the received signal. Due to the uncertainty in obtaining the actual modal response of BE, the frequency domain method should be used with caution.

3. Experimental Program and Methodology

Four (4) cylindrical undisturbed sand specimens (10 by 20 cm) were collected from boreholes advanced at different locations of the capital city (Abu Dhabi). The specimens were also collected from different depths of the boreholes. Routine geotechnical tests such

as moisture content, index densities, and gradation analysis were also conducted. Table 1 presents important properties of the materials representing the specimens. The specimens were extruded after splitting the tubes in halves and were then placed on the bottom platen. A rubber membrane was installed and a vacuum applied after attaching the top platen and O-rings. The specimen was allowed to consolidate in drained conditions before conducting dynamic testing.

Table 1. Material properties of samples.

Sample Name	Void Ratio	C _C	C _U	Material Description	Depth (m)	SPT-N Value
SA	0.81	0.82	2.45	Very dense, poorly graded sand with inclusions of crystalline gypsum	11–12	50
SB	0.72	1	2.00	Medium dense to very dense, poorly graded sand with silt and trace crystalline gypsum	1.5–2	21
SC	0.65	0.70	2.75	Medium dense, light grey to grey wet, non-plastic, silty sand, trace fine gravel, and shell fragments	4–5	17
SD	0.51	0.72	2.8	Medium dense to very dense, light brown to light grey wet, non-plastic, silty sand, trace fine gravel, and shell fragments	5–6	14

All tests were performed with cyclic triaxial (CT) equipment provided by VJ Tech (UK), following the ASTM standard (ASTM D3999-91, [20]). The bottom and top platens of the CT were fitted with bender elements (BE) of maximum input frequency of 10 kHz for low strain evaluation of Vs. Each specimen was tested at different effective confining pressures and in consolidated drained conditions. At each confinement, BE measurements were performed at an input frequency of 5 kHz due to better response at this frequency. At least 10 signals were stacked to enhance the signal-to-noise ratio. The measurements were repeated by inverting the polarity for better detection of shear wave arrivals. The Vs was finally calculated from the ratio of distance between the elements and the time interval between the trigger and first arrival.

Figure 1 presents the typical time histories of the signals recorded at the receiver (Rx). Typical Fourier spectra were also presented for the analysis of wavelength-to-specimen size ratios (e.g., Irfan et al. [6]; Cristiana et al. [19]). The energy of the propagating pulse was concentrated between 3 and 6 kHz, as shown in Figure 1b. The calculated wavelengths ranged from 3 to 10 cm, which ensured the presence of at least one wavelength within the distance (20 cm) between the transmitter and receiver to avoid near field effects (e.g., Arroyo [21]; Lee [22]). BE measurements were taken at seven confinements of 30, 40, 60, 80, 100, 120, 140 kPa. Figure 2 presents the typical receiver signals for some of the confinements.

CT testing was performed at 40, 100 and 140 kPa in displacement (stroke) control mode. The displacement was increased incrementally to measure the dynamic properties at different strain levels. An input signal of 1 Hz with 10 cycles was used in all tests to obtain raw hysteresis loops. The time signals of load and displacement were fitted with a simulated signal to generate symmetrical loops for further analysis (e.g., Kumar et al. [23]).

Figure 3a,b presents the measured and fitted signals for typical cyclic triaxial data. Figure 3c presents the comparison of hysteretic loops from measured and fitted signals. The load and displacement amplitudes in Figure 3a,b are normalized for clarity. The dynamic properties as a function of shear strain levels were then fitted with hyperbolic model presented in Equation (1).

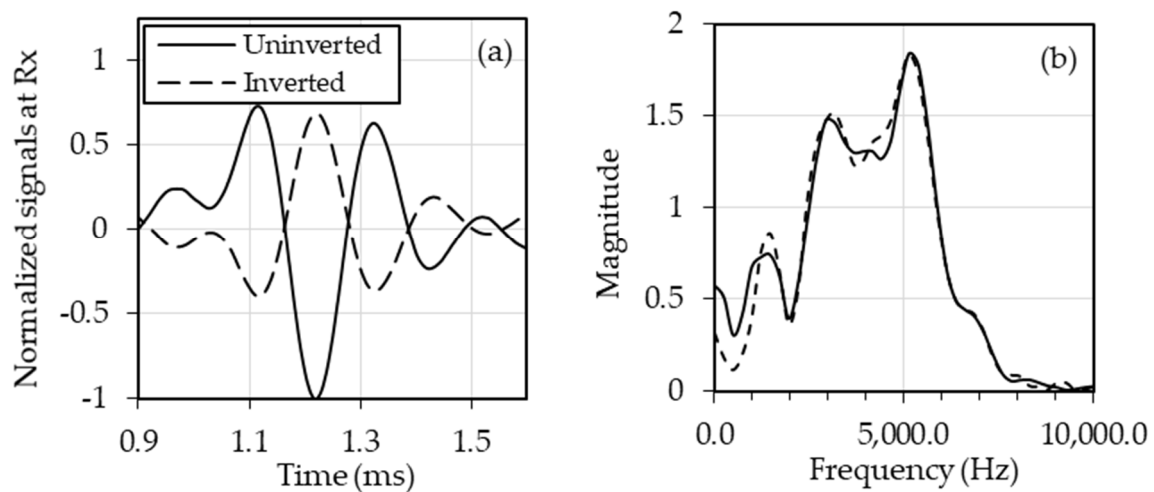


Figure 1. (a) Typical time history recorded at the Bender Element (BE) receiver (Rx) and (b) Fourier spectra of receiver signals.

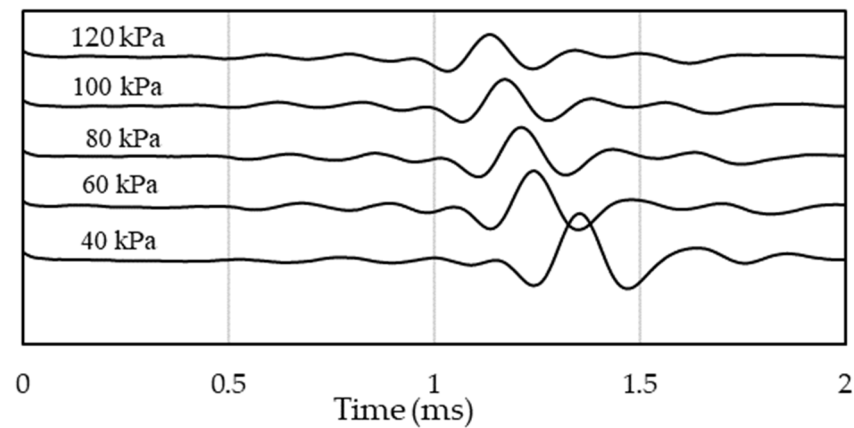


Figure 2. Typical receiver signals (staked) from the Bender Element testing at different confinements for sample SB.

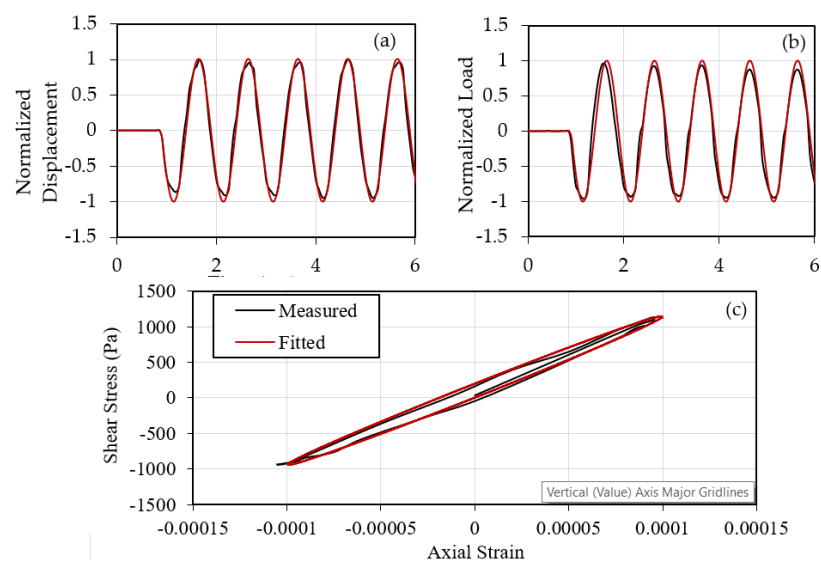


Figure 3. Typical measured and fitted functions for (a) displacement amplitude, (b) load amplitude, and (c) hysteresis loops (100 kPa).

Figure 4 illustrates the fitting of typical data from BE and CT tests with hyperbolic models. The data points at the lowest strain correspond to the results from the BE tests. The BE element data were assigned a shear strain value of 10^{-6} because it is difficult to calculate the strain level from the movement of the bender elements. The variation in lowest value of assigned shear strain was assumed to have a negligible effect on dynamic properties. The difference in frequency content between BE and CT tests is large; however, no study has suggested a model to correct for the frequency.

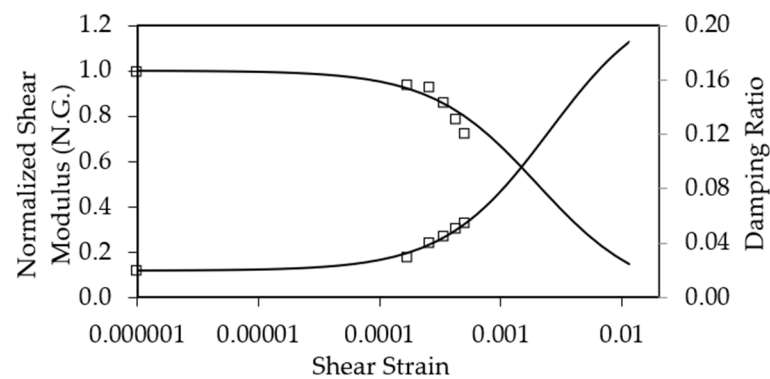


Figure 4. Illustration of hyperbolic models (Equation (1)) fitted to normalized shear modulus (N.G.) and damping ratio (sample SB, Confinement (σ) = 40 kPa).

A low-strain Poisson's ratio of uncemented to lightly cemented sands can range from 0.15 to 0.25, depending upon the saturation and cementation level (Santamarina et al. [24]). Fully saturated soil has a Poisson's ratio close to 0.5. CT typically evaluates the dynamic properties for medium to large strains; therefore, a value of 0.25 for the Poisson's ratio was selected for all conversions of elastic moduli (secant moduli) to shear moduli in this study. The sensitivity analysis showed that G will change by 8% only if the Poisson's ratio varies from 0.15 to 0.25. The damping ratios were calculated from standard procedures of analyzing hysteretic loops for energy stored and lost during one cycle (Equation (4)).

$$D = \frac{1}{4\pi} \frac{A_L}{A_T} \quad (4)$$

where A_L is the area of the loop, and A_T is the area under the line of secant modulus. The minimum damping ratios (D_{min}) corresponding to lowest shear strain levels were not measured (Figure 4). Evaluation of the low-strain damping ratio from BE and CT testing is difficult; therefore, a value of D_{min} was adopted, and a minimum shear strain level was assigned to it. Damping ratios decrease as the shear strain decreases, and then remains at a constant minimum value. The lowest damping in a best fit hyperbolic model represents D_{min} .

4. Results and Discussion

Figure 5a presents the variation of V_s with confinements for the tested samples. V_s values were normalized to the V_s value at the smallest confinement (30 kPa) for a better comparison in its trend with the confinements. Typically, a power model ($V_s = a\sigma^b$) is fitted to the variation of V_s with confinement (e.g., Cascante et al. [3]); therefore, Figure 5 also presents the exponents of the power models along with the data points to which the models are fitted. The coefficient of determination (r^2) of the power models was consistently larger than 0.9, except for sample SB ($r^2 = 0.77$). The general range of exponents (b), which defines the rate of increase in V_s with confinement, for silica sands ranged from 0.25 to 0.35, which were slightly larger than the results of most calcareous sands from this study. Lower values of exponents for calcareous sands are expected due to smaller stiffness at the inter-particle contacts due to the weaker calcite minerals compared to the silica minerals. Moreover, the

presence of gypsum in the sand deposits of ABD contribute to a weaker sand matrix when confinement increases (Table 1), especially in samples SA and SB. Figure 5a also shows that factors such as cementation at inter-particle contacts and inclusions such as seashells and a higher percentage of gypsum have a larger effect on the variation in V_s than the void ratio. Although smaller void ratio specimens (e.g., SC and SD) have a larger rate of increase in V_s , the trend is not clear when the results are compared with previous studies, as shown in Figure 5b.

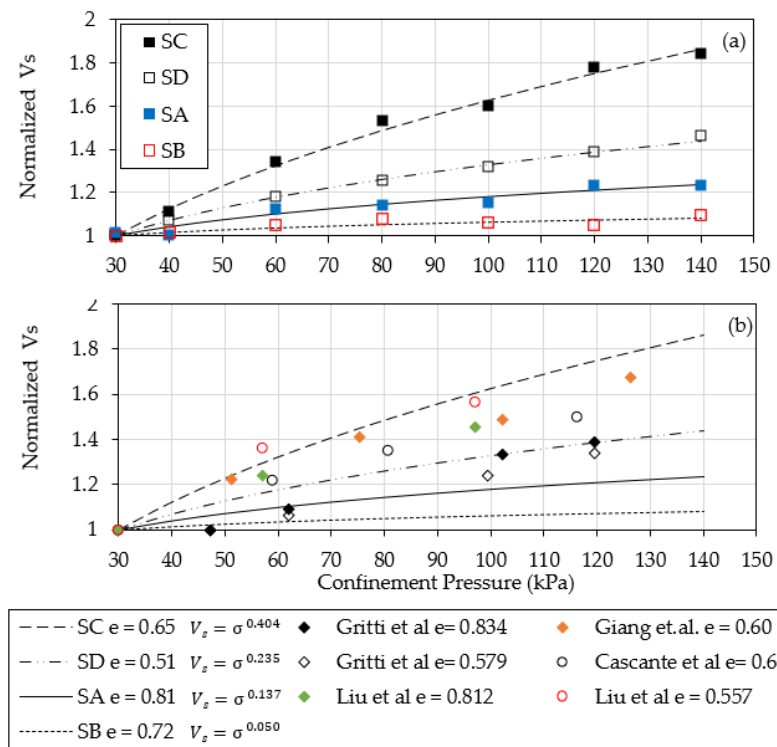


Figure 5. (a) Variation of normalized power models of shear wave velocity (V_s) with confinement (σ) for samples SA, SB, SC, and SD (data also shown). (b) Comparison of models with selected past studies on calcareous and silica sand (circular markers).

Figure 5b presents the comparison of power models with selected data for calcareous sands and for silica sands (circular markers) from the literature. Giang et al. [12] presented data for natural sand deposits of ABD; however, the samples were reconstituted. Although the void ratio of the sample SC was close to the sample of Giang et al. [12], the main focus of this study was not to evaluate the effect of the void ratio. The agreement between the sample SC and Giang et al. [12] is good at low confinements; however, the proposed models overestimate the data. The results from other studies at different void ratios are within the upper and lower bound for calcareous sands; however, a direct comparison based on void ratio is not appropriate due to reconstituted samples and different geographic regions. As noted earlier, the V_s of silica sand (circular markers) increases at a larger rate compared to most calcareous sands, of the present as well as of past studies.

Figure 6 presents the degradation of the shear modulus for the four samples at three confinement levels of 40, 100 and 140 kPa. Corresponding hyperbolic models of damping ratios are plotted on the secondary axes. The rate of degradation in all samples increases with a decrease in confinement. Samples SB and SC not only have slightly larger damping ratios but slightly larger increases in the damping ratio with shear strain. The trend can be attributed to the presence of seashells and traces of gypsum. Samples SB and SC were collected from shallow depths, and the degree of cementation at the inter-particle contacts is expected to be less than the samples from greater depths.

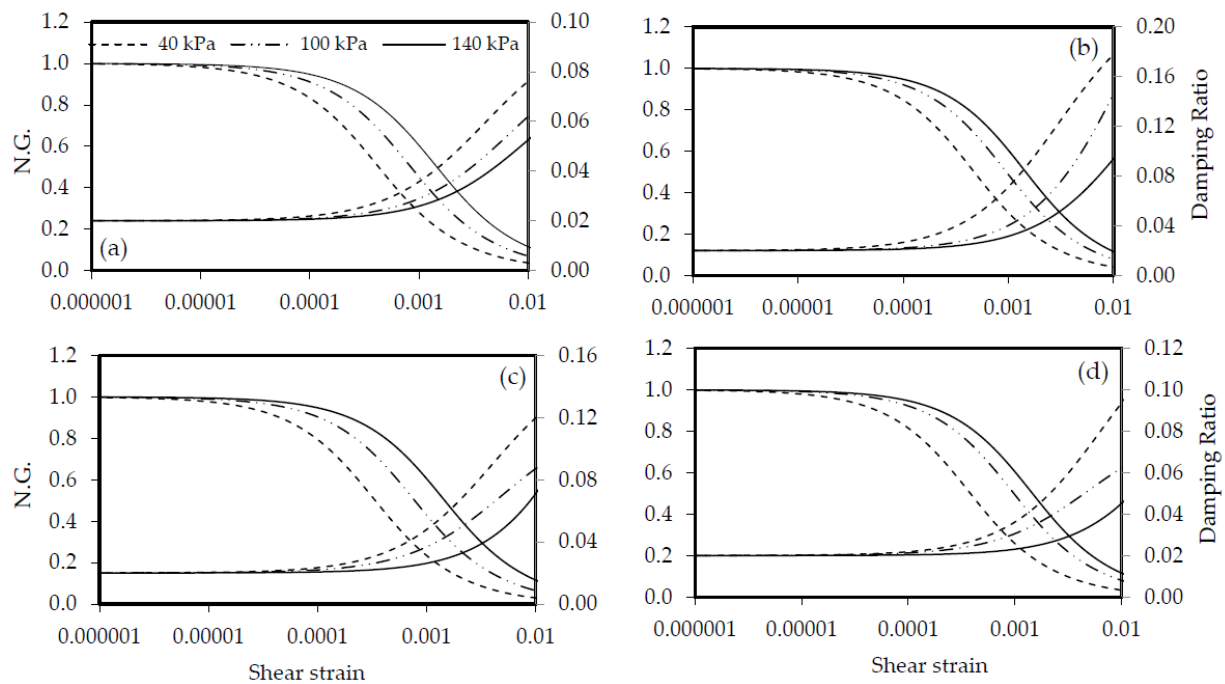


Figure 6. Proposed degradation models for normalized shear modulus (N.G.) and damping ratios for (a) sample SA; (b) sample SB; (c) sample SC; (d) sample SD.

The degradation behavior of the normalized shear modulus (N.G.) in Figure 6 appears to be independent of the type of sample and is almost identical at similar confinements. Damping ratios however are strongly influenced by the presence of varying and unpredictable degrees of cementation, which are prevalent in soil deposits found in ABD; however, large strains imposed during CT appear to mitigate this effect. Not all cementations that occur within the sand matrix are effective cementations (e.g., Lin et al. [25]). In undisturbed samples, the cementation can manifest as either effective (bridging of particles) that contributes to the stiffness or ineffective (grain coating or pore filling) that does not contribute to the stiffness (Lin et al. [25]; Dvorkin and Nur [26]).

Figure 7 presents the comparison of degradation models of all samples with selected degradation data from the literature on calcareous sands and one silica sand at 100 kPa. No study is available on the degradation behavior of soils for ABD, either for disturbed or undisturbed samples. The degradation behaviors for calcareous sands are however available for other regions, which are presented in Figure 7; albeit, the samples are reconstituted. The proposed degradation models from this study are similar at 100 kPa, which suggests that the degradation models presented in this study can be used for site response analysis in ABD, irrespective of its geographical location within urban ABD (Figures 7 and 8). The figure shows that the data from reconstituted samples of calcareous sands degrade quickly compared to the models from this study, especially at mid-strain levels (0.0001 to 0.001). The trend starts to converge at larger strains as a higher number of cemented contacts becomes ineffective.

The higher rate of decay in the dynamic properties for calcareous sands is indicative of micro-mechanical behavior that is also observed as a slower rate of increase in V_s with confinement. As the confinement increases or as the shear strain increases, the inter-particle matrix changes in a way that is different than silica sand. The degradation in the shear modulus and damping ratio of silica sand occurs at a noticeably slower rate (Figure 7). Calcareous sand may result in higher low-strain V_s values compared to silica sand; however, the change in conditions (confinement or strain) rearranges the inter-particle contacts in a different and least understood complex mechanism.

The comparison of damping ratios (Figure 7) indicates a similar trend; however, the low strain values from the literature are smaller. The higher damping ratios in the present

study can be attributed to the presence of inclusions such as seashells and gypsum, which can significantly increase the damping. The relatively smoother surface of shells increases the relative motion of the particles in contact with the shell, which contributes to an increase in localized strain. The presence of gypsum, which is less stiff than calcite, contributes to the damping ratio through larger viscous losses. In addition to these factors, most of the compared data points at low strains are obtained from the RC test, which is better than CT at evaluating the low-strain damping ratio. The equipment-generated damping ratio in the CT device has never been studied extensively, whereas numerous mathematical and experimental procedures are published to correct the damping ratio in the RC device (e.g., [3,5]).

Figure 8 separately compares the proposed degradation models with results from Jaafarian et al. [9] at a confinement of 40 kPa. The data at a confinement of 100 kPa from Jaafarian et al. [9] are not available. Figure 8 also indicates that the trends in the degradation models for the tested samples are comparable at 40 kPa. The rate of decay of the proposed hyperbolic models is smaller than the data from Jaafarian et al. [9], which corroborate the comparisons and discussions presented in the context of 100 kPa (Figure 7).

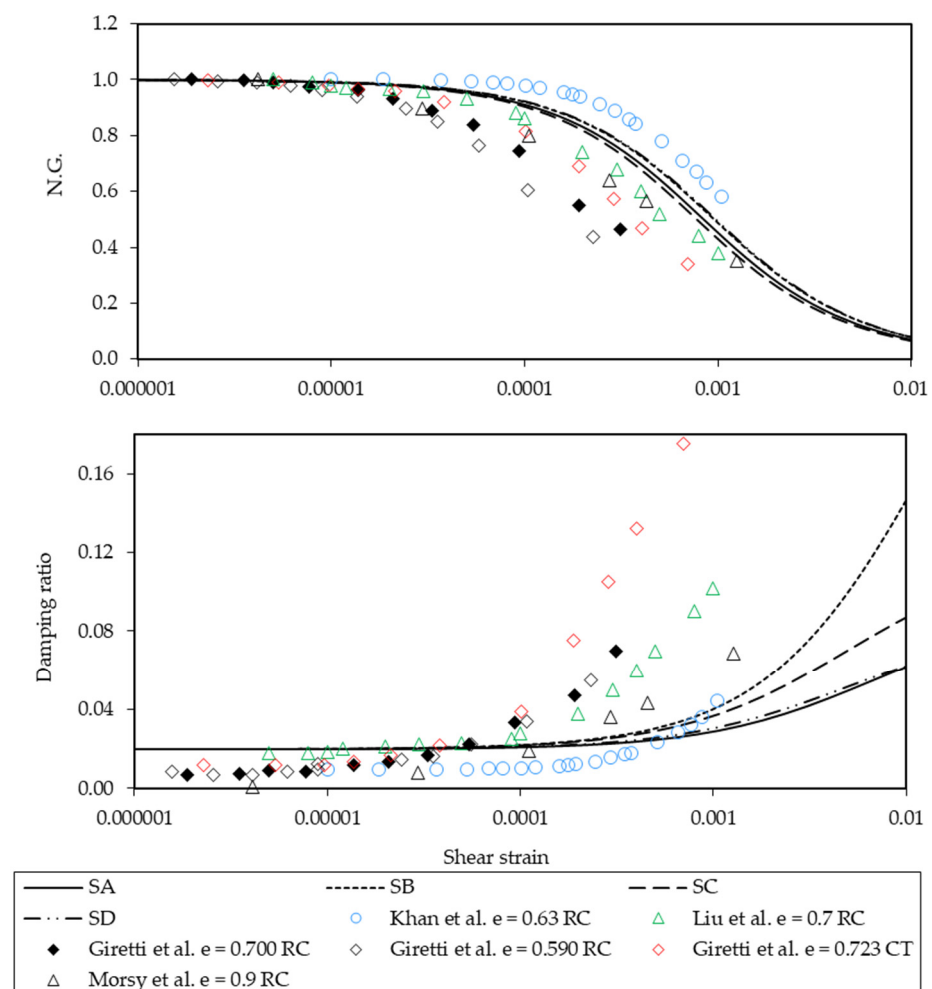


Figure 7. Comparison of proposed degradation models with selected studies on calcareous and silica sands at $\sigma = 100$ kPa from cyclic triaxial (CT) and resonant column (RC) tests. Silica sand data are represented with circular markers.

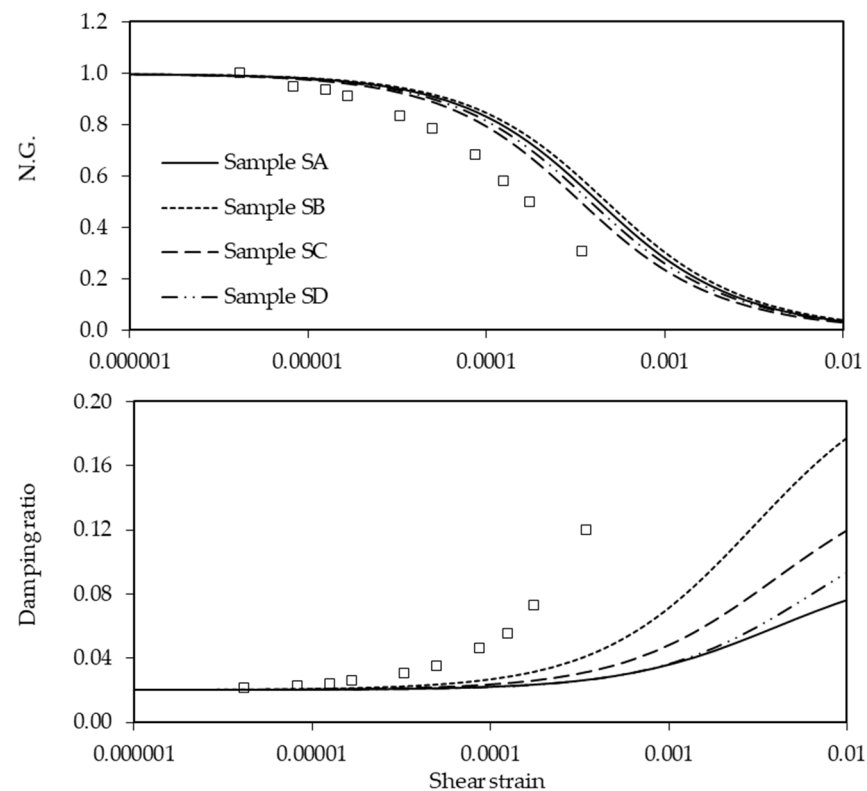


Figure 8. Comparison of proposed degradation models from the study by Jafarian et al. [9] on calcareous sand at Confinement (σ) = 40 kPa from resonant column (RC) testing.

5. Conclusions

ABD has developed its own national building code that requires a dynamic analysis of structures for seismic loadings. Although low-strain dynamic properties of in situ sand deposits that are rich in carbonate minerals are available, no study has presented the degradation models of the dynamic properties for in situ undisturbed soil samples for ABD. This study presented the results of dynamic testing on undisturbed soil samples taken from different sites of urban ABD. Bender element (BE) and cyclic triaxial (CT) tests were performed for low-strain and large-strain characterization of calcareous sand deposits within urban ABD. The results were curve-fitted with power and hyperbolic models and then compared with studies on selected calcareous and silica sands from the literature. The main conclusions from the present study are presented in the following.

- The rate of increase in V_s with confinement for carbonate sands varied significantly and strongly depended on the sand matrix and its inclusions. The presence of cementation, seashells, and other minerals such as gypsum caused large variability among the samples. Low-strain values of V_s and its variation with confinement must be evaluated on a case-by-case basis.
- The large strain behavior (degradation of dynamic properties) was similar for all tested sand samples at equivalent confinements, irrespective of their spatial distribution in ABD. The degradation models presented in this study can therefore be used for dynamic analysis of the structures under seismic loading or site response analysis. The rate of degradation for calcareous sands tested in the present study was larger than for silica-based sands.
- The rate of degradation of dynamic properties in undisturbed samples of calcareous sands was smaller in comparison to previous studies on calcareous sands. A larger degradation in previous studies, especially at mid-strains, was mainly attributed to the remolding of samples, which can disturb the cementation at inter-particle contacts. At very large strains however, the comparisons converged.

- The damping ratios of the tested samples were larger for the smaller strains in comparison to the previous studies due to a different testing device (RC), larger localized strains, and the presence of gypsum. At larger strains however, the tested samples in the present study indicate damping ratios that are smaller than other studies on similar sands.

Author Contributions: Conceptualization, Z.H.K., A.K. and M.A.; methodology, Z.H.K., A.K. and K.F.; software, A.K.; validation, Z.H.K., M.A. and K.F.; formal analysis, A.K. and Z.H.K.; investigation, Z.H.K. and A.K.; resources, M.A., Z.H.K., M.E.E. and K.F.; data curation, Z.H.K., A.K. and M.A.; writing—original draft preparation, A.K. and Z.H.K.; writing—review and editing, Z.H.K., M.A. and K.F.; visualization, A.K., Z.H.K. and M.A.; supervision, Z.H.K., M.A., M.E.E. and K.F.; project administration, Z.H.K.; funding acquisition, Z.H.K., M.A. and M.E.E. All authors have read and agreed to the published version of the manuscript.

Funding: This research was funded by The American University of Sharjah, grant number FRG19-M-E08. The work in this paper was supported, in part, by the Open Access Program from the American University of Sharjah.

Institutional Review Board Statement: Not applicable.

Informed Consent Statement: Not applicable.

Data Availability Statement: Not applicable.

Acknowledgments: The authors would like to acknowledge the support of machine shop at the American University of Sharjah for the manufacturing of extraction tools for the samples.

Conflicts of Interest: The authors declare no conflict of interest. The funders had no role in the design of the study; in the collection, analyses, or interpretation of data; in the writing of the manuscript, or in the decision to publish the results. This paper represents the opinions of the author(s) and does not mean to represent the position or opinions of the American University of Sharjah.

References

1. Abu Dhabi International Building Code (ADIBC) 2014; Department of Municipal Affairs: Abu Dhabi, United Arab Emirates, 2014.
2. Kirkham, A. Pleistocene Carbonate Seif Dunes and their Role in the Development of Complex Past and Present Coastlines of the U.A.E. *GeoArabia* **1998**, *3*, 19–32. [\[CrossRef\]](#)
3. Cascante, G.; Vanderkooy, J.; Chung, W. A new mathematical model for Resonant-Column measurements including eddy-current effects. *Can. Geotech. J.* **2005**, *42*, 121–135. [\[CrossRef\]](#)
4. Khan, Z.; Cascante, G.; El Naggar, M.; Lai, C. Measurement of Frequency-Dependent Dynamic Properties of Soils Using the Resonant-Column Device. *J. Geotech. Geoenviron. Eng.* **2008**, *134*, 1319–1326. [\[CrossRef\]](#)
5. Khan, Z.; Cascante, G.; Moayerian, S.; Grabinsky, M. Evaluation of transfer function and dynamic properties from strain-controlled Resonant Column tests. *Geotech. Test. J.* **2013**, *36*, 1–8. [\[CrossRef\]](#)
6. Irfan, M.; Cascante, G.; Basu, D.; Khan, Z. Novel Evaluation of Bender Element Transmitter Response in Transparent Soil. *Géotechnique* **2020**, *70*, 187–198. [\[CrossRef\]](#)
7. Carraro, H.; Bortolotto, S. Stiffness degradation and damping of carbonate and silica sands. In *Frontiers in Offshore Geotechnics III*; Taylor and Francis Group: London, UK, 2015; pp. 1179–1183.
8. Fioravante, V.; Jamiolkowski, M.; lo Presti, F. Stiffness of carbonatic Quiou sand. In Proceedings of the International Conference on Soil Mechanics and Foundation Engineering, New Delhi, India, 5–10 January 1994; pp. 163–167.
9. Jafarian, Y.; Javdanian, H.; Haddad, A. Strain-dependent dynamic properties of Bushehr siliceous-carbonate sand: Experimental and comparative study. *Soil Dyn. Earthq. Eng.* **2018**, *107*, 339–349. [\[CrossRef\]](#)
10. Liu, X.; Li, S.; Sun, L. The study of dynamic properties of carbonate sand through a laboratory database. *Bull. Eng. Geol. Environ.* **2020**, *79*, 3843–3855. [\[CrossRef\]](#)
11. Van Impe, P.O.; Van Impe, W.F.; Manzotti, A.; Mengé, P.; Van Den Broeck, M.; Vinck, K. Compaction control and related stress-strain behaviour of off-shore land reclamations with calcareous sands. *Soils Found.* **2015**, *55*, 1474–1486. [\[CrossRef\]](#)
12. Giang, P.H.; Van Impe, P.O.; Van Impe, W.F.; Menge, P.; Haegeman, W. Small-strain shear modulus of calcareous sand and its dependence on particle characteristics and gradation. *Soil Dyn. Earthq. Eng.* **2017**, *100*, 371–379. [\[CrossRef\]](#)
13. Giretti, D.; Fioravante, V.; Been, K.; Dickenson, S. Mechanical properties of a carbonate sand from a dredged hydraulic fill. *Géotechnique* **2018**, *68*, 410–420. [\[CrossRef\]](#)
14. Hardin, B.O.; Drnevich, V.P. Shear Modulus and damping in soils: Design equations and curves. *J. Soil Mech. Found. Div.* **1972**, *98*, 667. [\[CrossRef\]](#)

15. Morsy, A.M.; Salem, M.A.; Elmamlouk, H.H. Evaluation of dynamic properties of calcareous sands in Egypt at small and medium shear strain ranges. *Soil Dyn. Earthq. Eng.* **2019**, *116*, 692–708. [[CrossRef](#)]
16. Hardin, B.O. The 6. Nature of Damping in Sands. *J. Soil Mech. Found. Div.* **1965**, *91*, 63–97. [[CrossRef](#)]
17. Brocanelli, D. Measurement of low-strain material damping and wave velocity with bender elements in the frequency domain. *Can. Geotech. J.* **1998**, *35*, 1032–1040. [[CrossRef](#)]
18. Camacho-Tauta, J. Experimental and Numerical Observations of the Frequency-Domain Method in Bender-Element Testing. *J. Geotech. Geoenviron. Eng.* **2017**, *143*, 4016–4096. [[CrossRef](#)]
19. Cristiana, F.; Díaz-Durán, F.; Fonseca, A.V.; Cascante, G. New Approach to Concurrent Vs and VP Measurements Using Bender Elements. *ASTM Int.* **2021**, *44*, 20200207.
20. ASTM D3999-91; Standard Test Methods for the Determination of the Modulus and Damping Properties of Soils Using the Cyclic Triaxial Apparatus. Annual Book of Standards. American Society for Testing and Materials: West Conshohocken, PA, USA, 2012.
21. Arroyo, F. Source near-field effects and pulse tests in soil samples. *Géotechnique* **2003**, *53*, 337–345. [[CrossRef](#)]
22. Lee, J.S. Bender Elements: Performance and Signal Interpretation. *J. Geotech. Geoenviron. Eng.* **2005**, *131*, 1063–1070. [[CrossRef](#)]
23. Kumar, S.S.; Murali, A.K.; Dey, T.A. Evaluation of Hysteretic Damping of Sand at Large Shear Strains using Cyclic Triaxial Tests. In Proceedings of the Geotechnics for Natural and Engineered Sustainable Technologies: Indian Geotechnical Conference (GeoNEst: IGC-2017), Guwahati, India, 14–16 December 2017.
24. Santamarina, J.C.; Rinaldi, V.A.; Fratta, D.; Klein, K.A.; Wang, Y.H.; Cho, G.C.; Cascante, G. A Survey of Elastic and Electromagnetic Properties of Near-Surface Soils. *Near-Surf. Geophys.* **2005**, *1*, 71–87.
25. Lin, H.; Suleiman, M.T.; Brown, D.G. Investigation of pore-scale CaCO₃ distributions and their effects on stiffness and permeability of sands treated by microbially induced carbonate precipitation (MICP). *Soils Found.* **2020**, *60*, 944–961. [[CrossRef](#)]
26. Dvorkin, J.; Nur, A. Elasticity of high-porosity sandstones: Theory for two North Sea data sets. *Geophysics* **1996**, *61*, 1363–1370. [[CrossRef](#)]